COMPARATIVE HIGH-TEMPERATURE OXIDATION TESTS WITH ZIRCALOY-4 IN VARIOUS ATMOSPHERES

MARTIN STEINBRÜCK, PHILIPP VAN APPELDORN

Karlsruhe Institute of Technology, Institute for Applied Materials IAM-AWP
Hermann-von-Helmholtz-Platz 1, 76344 Eggenstein-Leopoldshafen – Germany

ABSTRACT

This study presents results of overall 124 oxidation tests of Zircaloy-4 at 900°C, 1000°C and 1100°C in different nitrogen-containing atmospheres, namely air (oxygen-nitrogen), steam-nitrogen, steam-air, and, for comparison, pure steam under comparable boundary conditions. The experiments were conducted in a tube furnace coupled with a sophisticated gas/steam inlet system and a mass spectrometer to analyse the composition of the off-gases. The experiments confirmed the strong effect of nitrogen on the oxidation of zirconium alloys. Metallographic post-test examinations were conducted mainly using optical microscopy. The oxidation kinetics of Zircaloy-4 in atmospheres containing nitrogen was similar to each other, but was much faster compared to reference tests in pure steam. Initial local attack of nitrogen was observed for all gas mixtures containing nitrogen, whereas the oxide scale formed under steam atmosphere developed homogeneously.

1. Introduction

Most investigations of core degradation during nuclear reactor accidents have considered oxidation of metal core components, mainly of zirconium alloy cladding tubes, by steam only [1]. However, there are various scenarios where air or nitrogen may have access to the core [2]. Air ingress is possible under shutdown conditions when the reactor coolant system is open to the containment atmosphere. Air oxidation of the remaining outer core regions after reactor pressure vessel failure in the late phase of core degradation during severe accidents was identified to be another possible scenario. Furthermore, spent fuel pool (SFP) accident scenarios including air ingress have attracted attention especially after the Fukushima Daiichi accidents [3]. Nitrogen is used for inertisation of reactor containments in boiling water reactors and for pressurising emergency core cooling systems (ECCR) [4].

Experiments in air and other, more prototypic, gas mixtures containing nitrogen have shown a strong influence of nitrogen on the oxidation kinetics and hence on degradation of cladding tubes and, if steam is available, on hydrogen source term [5] - [15]. Furthermore, a strong dependence of oxidation kinetics on the thermo-hydraulic boundary conditions (flow rates, gas partial pressures, etc.) was observed [16]. Usually, a transition takes place from initially (sub-)parabolic kinetics determined by oxygen (vacancy) diffusion through a dense protective oxide scale to rather linear kinetics determined by gas phase diffusion through a porous oxide layer. The accelerating effect of nitrogen on the oxidation kinetics is caused by the temporary formation of zirconium nitride, ZrN, and its re-oxidation connected with large changes of molar volumes of the involved phases and with it the formation of strongly porous oxide scales.

Zirconium nitride, obviously playing a prominent role in the reaction mechanism, is (1) only stable at very low oxygen partial pressure, practically in the absence of oxygen, and (2) forms fastest during the reaction of oxygen-saturated zirconium with nitrogen [17]. Both conditions, the thermodynamic and the kinetic one, are fulfilled locally at the metal-oxide

interface or globally during oxygen/steam starvation conditions. Lasserre et al. [12] have shown that the nitrogen attack starts locally and they proposed a model based on nucleation and growth of ZrN-affected regions [18]; but the model development was based on limited data of tests only at 850°C.

Most experiments performed in the past were conducted in thermogravimetric systems allowing in-situ measurement of mass changes, but providing only the end status of one sample for post-test examinations. The experiments presented in this paper were conducted in a horizontal tube furnace coupled with a mass spectrometer delivering in-situ data of the off-gas composition. Three temperatures below and above the so-called breakaway regime for zirconium oxidation [19] were chosen, namely 900, 1000, and 1100°C. The experiments were conducted in four different atmospheres: (1) air, (2) steam-nitrogen, (3) steam-air, and (4) steam as reference. The paper provides mass gain data, results of mass spectrometric analysis of the gas composition as well as outcomes of macroscopic and microscopic post-test examinations.

2. Experimental details

2.1 Test setup and samples

All tests were conducted at normal pressure in a horizontal tube furnace (LORA-1800) with a sample lock allowing fast change of samples with the furnace staying at the test temperature. The inner diameter of the alumina reaction tube is 32 mm. Gas and steam flow rates are controlled by Bronkhorst® gas and liquid flow controllers and a controlled evaporator and mixing (CEM) system. The furnace is coupled with a mass spectrometer (Balzers GAM300) for quantitative analysis of the off-gas composition including the following species: H_2, O_2, N_2, H_2O, and Ar. For the isothermal tests in steam, the specimens were shifted from the air lock filled with argon into the furnace at test temperature in flowing inert argon atmosphere. After approx. 1 min for temperature homogenization, the reactive gas mixture including steam was injected in axial sample direction. After the predefined time at constant temperature, the steam+gas was switched off, and the specimen was removed simultaneously from the heated zone of the furnace and cooled in the air lock in argon for approx. 5 min to room temperature. During the experiments in (non-condensable) air, a steady air-argon gas mixture was flowing through the reaction tube during the whole test series.

Zircaloy-4 samples, 2 cm long, were cut from commercial cladding tubes (10.75 mm external diameter, 0.75 mm thickness), deburred, and cleaned in an ultrasonic bath with isopropanol and dried in hot air.

2.2 Test conditions

Altogether 124 experiments were conducted at temperatures of 900, 1000, and 1100°C under four different atmospheres, namely (1) synthetic air, (2) steam-nitrogen, (3) steam-air, and (4) steam for reference. The nominal flow rates given in Table 1 have been chosen to be comparable with respect to the oxygen supply available for oxidation.

Argon was used as carrier gas for the steam production in the CEM and as reference gas for quantitative gas analyses by mass spectrometry.
For each condition 8-10 experiments have been conducted with 1 to 90-180 min duration in order to get sufficient information about the oxidation kinetics. The maximum test duration was reached latest when the sample was completely oxidised.

Atmosphere	H_2O, g/h	O_2, l/h	N_2, l/h	Ar, l/h
Synthetic air	-	10	40	20
Steam-nitrogen	16.1	-	40	20
Steam-air	16.1	5	20	20
Steam	16.1	-	-	20

Table 1: Nominal flow rates (at standard conditions) of gases for the various atmospheres applied

2.3 Measurements and post-test examinations

The mass of each sample before and after tests was determined using an analytical balance with an accuracy of 0.1 mg. In the framework of this study, macro photos were taken of each sample in order to document the general post-test appearance of the samples and especially their surfaces. Then, the samples were embedded into epoxy resign, cut in the middle position, ground and finally polished. Micrographs of the samples were taken with various magnifications. Gas concentrations measured by mass spectrometer were converted into flow rates using the argon flow rate as reference.

The samples are now available for more sophisticated analyses like SEM/WDX, Raman spectroscopy, EBSD or TEM methods.

3. Results

3.1 Mass gain

Mass gain data of all tests are summarised in the diagrams given in Figure 1. At first glance a significant difference between the nitrogen containing atmospheres and steam is visible for all temperatures. After an initial period with comparable mass gains, the kinetics strongly increased for the tests in nitrogen-containing atmospheres after approx. 60 min, 20 min and almost from the beginning for the test series at 900, 1000, and 1100°C, respectively. Hence, these results confirm former studies on the effect of nitrogen on the oxidation kinetics of zirconium alloys with respect to the early transition from protective to non-protective oxide scale formation and the corresponding change in rate law connected with strong increase of the oxidation rates after the transition. The reaction follows roughly linear rate laws for all temperatures and atmospheres at 900 and 1000°C after transition and at 1100°C almost from the beginning until complete oxidation is approached (35 wt% or 833 g/m^2 for this sample geometry).

Most significant at 900°C, the highest mass gains, and hence oxidation rates, are measured for the samples oxidised in steam-nitrogen mixture. This effect is also seen at the higher temperatures, but less pronounced. The mass gain data obtained for the samples in pure steam are in accordance with the well accepted correlation by Cathcart and Pawel (CP) [20], especially at 1000°C until beginning of breakaway beyond 120 min and at 1100°C. The parabolic CP correlation overestimates the mass gain data of the 900°C series. At this temperature, rather a cubic rate law is expected for the oxidation of zirconium alloys [13].

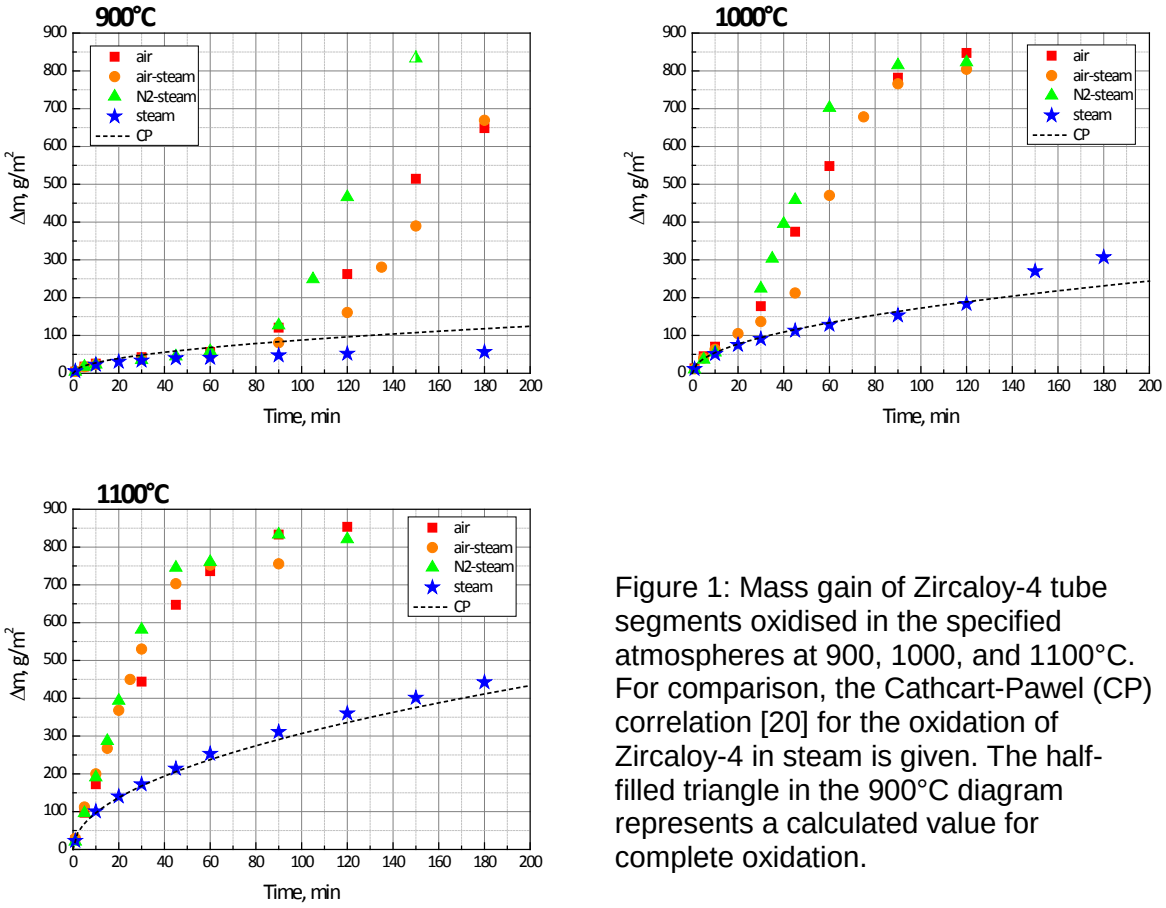

Figure 1: Mass gain of Zircaloy-4 tube segments oxidised in the specified atmospheres at 900, 1000, and 1100°C. For comparison, the Cathcart-Pawel (CP) correlation [20] for the oxidation of Zircaloy-4 in steam is given. The half-filled triangle in the 900°C diagram represents a calculated value for complete oxidation.

3.2 Off-gas composition

In-situ mass spectrometer measurement including all relevant gas species were performed during the oxidation experiments. Figure 2 gives examples of mass spectrometer results obtained during 2-hours lasting experiments at 1000°C providing interesting insight into the reaction mechanisms. Generally, all tests, including the ones at 1100°C, did not show any evidence of starvation conditions for steam or oxygen, i.e., only relatively low amounts of the injected gases were consumed by the reaction with the samples. Also, the overall behaviour was similar for all temperatures, but reflecting increased reaction rates with rising temperature.

The mass spectrometer results of the test in air (Figure 2a) show almost constant flow rates of oxygen and nitrogen during the whole experiment. More magnified curves (Figure 2c) reveal consumption of oxygen initially and between approx. 30 and 90 min as well as consumption of nitrogen between approx. 25 and 70 min and release of nitrogen from approx. 70 to 110 min. This observation fits well with the mass gain progress (Figure 1) showing high rates at 1000°C between 30 and 90 min when (almost) complete oxidation is obtained. A similar behaviour is observed for the reactions in steam-air with regard to the oxygen and nitrogen release rates. Interestingly, no hydrogen is detected in the off-gas, although steam is also consumed initially and between 30 and 60 min, see Figure 2d. The hydrogen produced by this reaction must be absorbed by the metal. Its release towards the end of the experiment approaching complete oxidation is not seen in the mass spectrometer results because it reacts in-situ with oxygen forming water molecules. Indeed, a slight increase of the steam flow rate towards the end of the experiment is seen by the inserted dashed linear fit line in the diagram.

Significant hydrogen release was measured during the experiments in steam and steam-nitrogen. Both hydrogen flow rate curves in Figure 2e+f feature an initial peak followed by slowdown of the hydrogen production and again an increase after transition to non-protective oxide scale formation. Whereas the initial hydrogen peaks are comparable for the two tests resulting in maximum release rates of approx. 25 l/h, the timing and magnitude of the second peak are significantly different. The transition in the steam-nitrogen atmosphere starts considerably earlier (after 20 min compared to 120 min in steam) and results in twenty times higher hydrogen release rates. A closer view on the nitrogen release rates during the steam-nitrogen tests reveals a similar behaviour as in the steam-air tests, i.e., first consumption and later release of nitrogen by the sample.

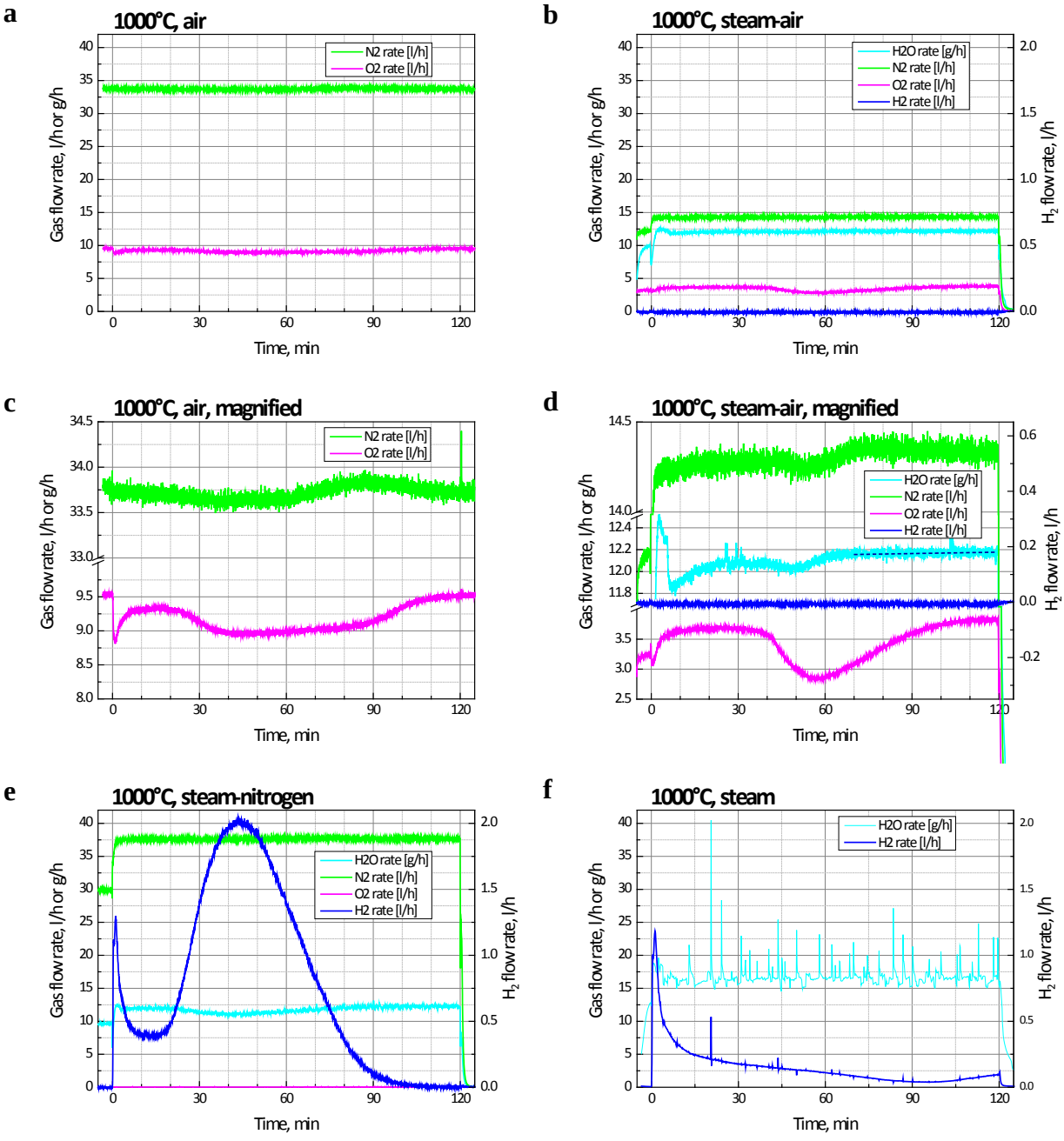

Figure 2: Gas flow rates calculated from mass spectrometer measurements during experiments for 2 hours at 1000°C in the specified atmospheres.

3.3 Post-test examinations

A representative selection of macro-photos showing the appearance of the samples after oxidation at the conditions specified is presented in Figure 3-Figure 5. These images confirm the mass gain and gas analysis results showing much stronger degradation of the samples annealed in nitrogen-containing atmospheres compared to the ones oxidised in steam. Depending on temperature, first light spots are visible for the samples which have seen nitrogen after a certain time. Later on, an increasing network of cracks developed at these samples before a more or less complete oxidation of the sample surface, and as deduced from the mass gain data, of the volume, took place. On the contrary, the surfaces of the steam-oxidised samples look homogeneous except the one annealed for two hours at 1000°C featuring spalled oxide scales due to the breakaway oxidation.

A significant volume increase with progressing oxidation was observed for the samples in nitrogen-containing atmospheres. The colour of the samples' surfaces varies between the different atmospheres. It is typically dark and shiny for dense, adherent oxide scale regions and light-coloured for porous and less adherent oxide. The comparably darker surface colour of most samples oxidised in steam-nitrogen is remarkable.

Figure 3: Post-test appearance of samples oxidised at 900°C in specified atmospheres.

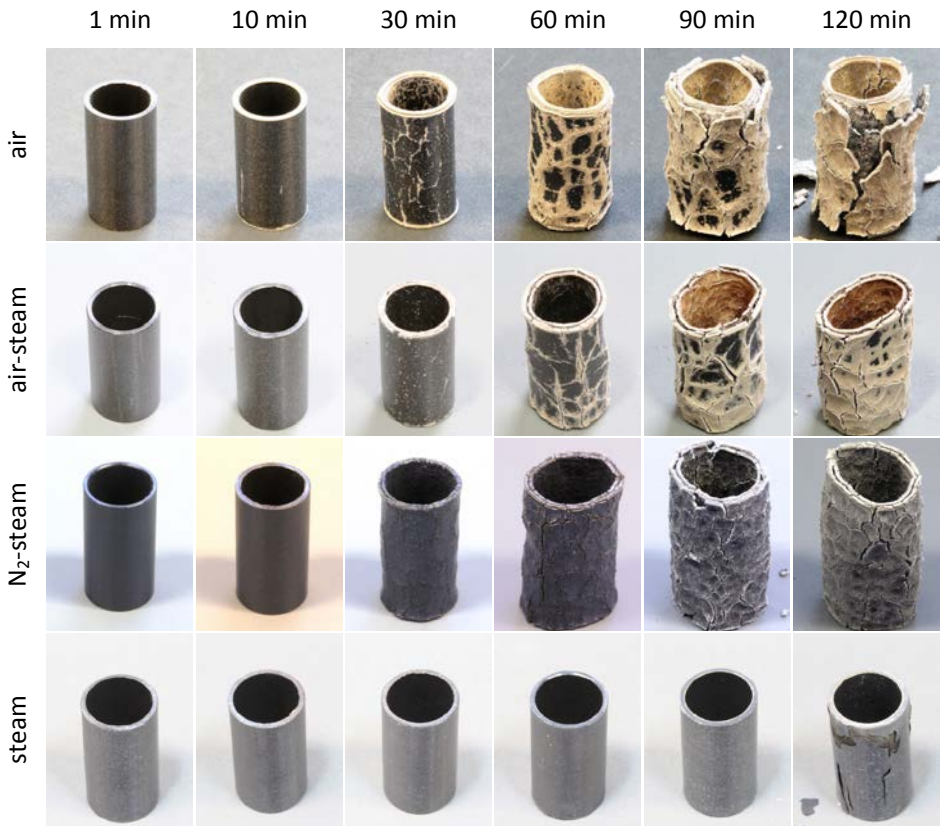

Figure 4: Post-test appearance of samples oxidised at 1000°C in specified atmospheres.

Figure 5: Post-test appearance of samples oxidised at 1100°C in specified atmospheres.

Many micrographs of the sample cross sections were taken. Here only a limited selection can be provided illustrating the main features of the Zircaloy-4 oxidation under the different

atmospheres. The micrographs give more detailed information of the nature of the initially local attack of nitrogen and the spreading of the affected areas through the whole samples. Figure 6 provides snapshots of the samples' cross sections of the test series at 1100°C in steam-nitrogen atmosphere. The different appearance of the inner and outer surface of the tube segments is obvious and will be discussed in the next section. Contrary to the external surface the internal one seems to be attacked more homogeneously. This effect was most pronounced for all samples in nitrogen-containing atmospheres at 1100°C and less significant at the lower temperatures.

The further presentation here will concentrate on the more prototypic external oxidation. The locally beginning enhanced oxidation is clearly connected with the formation of the golden-coloured zirconium nitride phase, ZrN, which is preferably seen near the metal-oxide interface. First local nodular areas with nitride formation and corresponding porous oxide scale are already visible after 5 min oxidation. But most of the external surface is still covered by a thin adherent and dense oxide. The nitride "nests" increase with respect to number and size with progressing oxidation time and finally cover the whole sample surface. After 60 min only oxide and internal nitride is visible which is also re-oxidised and converted after 120 min. It is not clear what is the reason for the initial nitrogen attack; most probably any imperfection in the initially formed oxide scale may act as nucleation point.

This general behaviour was observed for all nitrogen-containing atmospheres at all temperatures with the tendency of strongest oxidation for the samples oxidised in steam-nitrogen, hence confirming the mass gain results. With lower temperatures, the expansion of the mixed ZrO_2/ZrN zones near the metal-oxide interface as well as the ZrN grain sizes decreased.

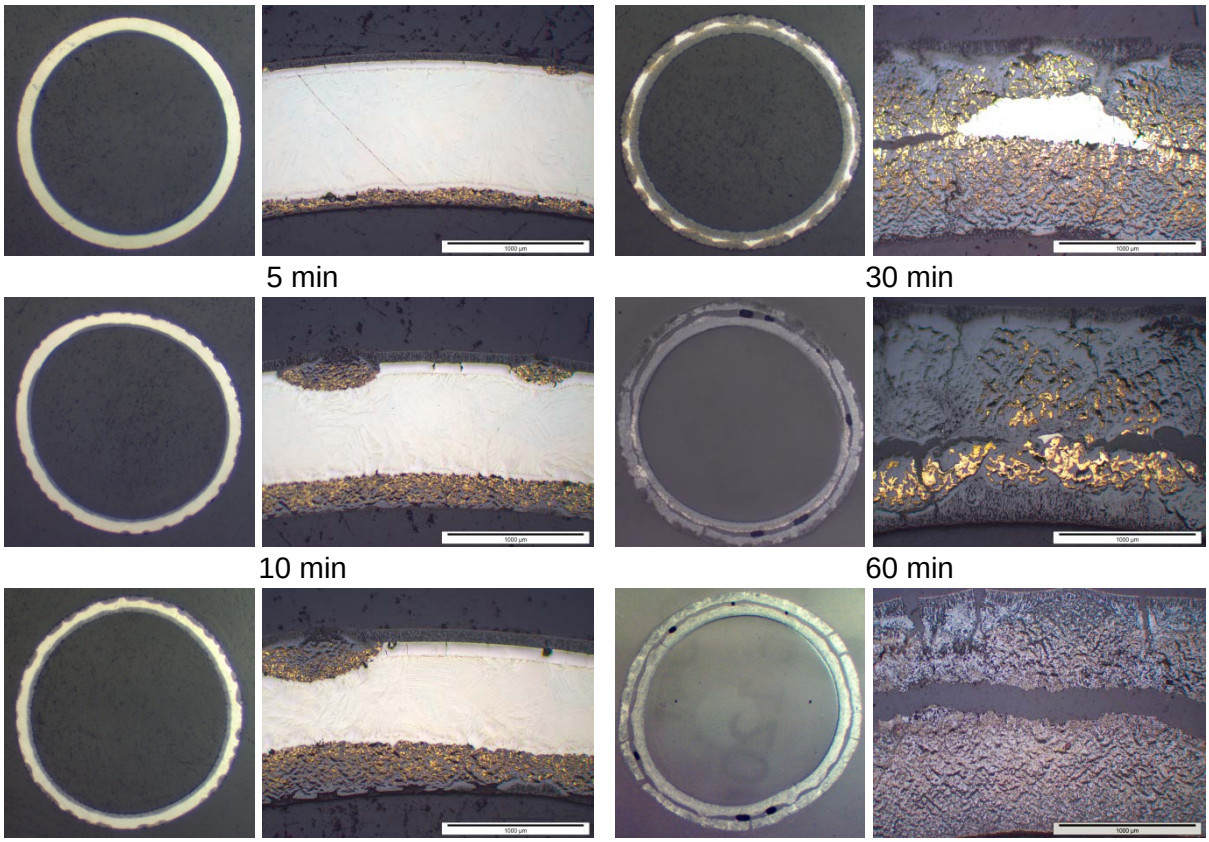

Figure 6: Macrographs (not to scale among each other) and micrographs of sample cross sections after oxidation at 1100°C in steam-nitrogen atmosphere. The involved phases are the bright Zr(O) metal, the grey oxide ZrO_2 and the golden-coloured nitride ZrN. The scale bar in the micrographs corresponds to 1000 µm.

This can be seen for instance in Figure 7 providing comparative micrographs of samples oxidised for 45 min at 1000°C under the four different atmospheres. The samples oxidised in nitrogen-containing atmospheres are strongly degraded with all features already discussed: locally inhomogeneous oxidation, nitride formation near the metal-oxide interface, and strongest oxidation in the steam-nitrogen mixture. Contrary, the sample oxidised in steam is covered by a dense and adherent oxide scale followed by oxygen-stabilised α-Zr(O) with most of the metal left (former β-Zr).

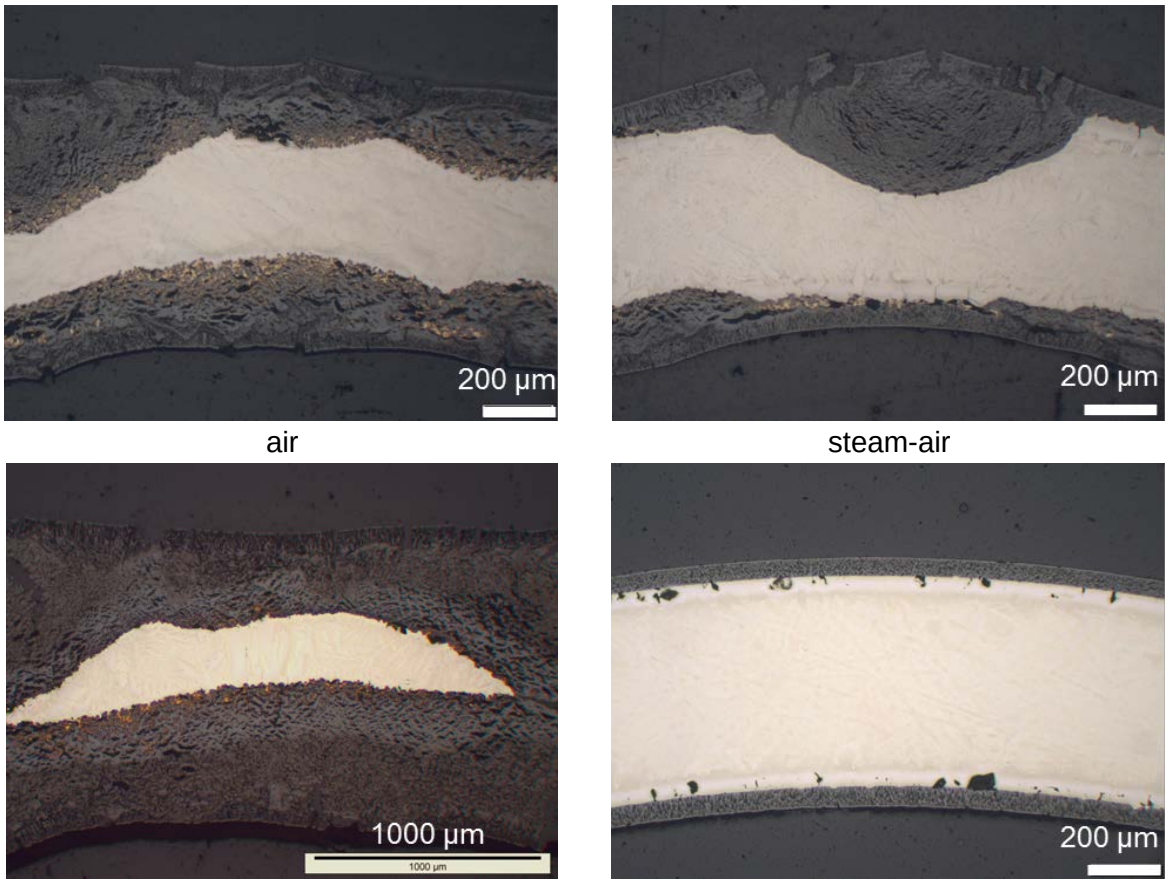

air steam-air

steam-nitrogen steam

Figure 7: Micrographs of sample cross sections after 45 min oxidation at 1000°C in the specified atmosphere.

4. Discussion

The experimental results presented in this paper clearly confirm the crucial role of nitrogen on the oxidation mechanisms and kinetics of zirconium alloys. The mechanisms are well known and documented in many papers as summarised in the introduction. Hence, the discussion here will focus on the special outcome of the presented experiments.

The use of a mass spectrometer for analysing the off-gas composition gave some interesting insights. So, the consumption of nitrogen by the formation of zirconium nitride was seen as well as its release during the re-oxidation of ZrN towards complete oxidation. Thermodynamically, zirconium nitride is only stable at very low oxygen partial pressure, practically in the absence of oxygen [17]. As long as metal phase is available, the local oxygen partial pressure at/near the metal-oxide interface is determined by the Zr/ZrO_2 equilibrium. With increasing distance from this interface, and latest when the metal phase is completely consumed, the oxygen partial pressure increases and leads to the re-oxidation of the remaining zirconium nitride connected with N_2 release.

Even more interesting is the hydrogen signal during the experiments including steam. As seen in Figure 2 hydrogen was produced and released, as expected, in steam and steam-nitrogen atmosphere, but definitely not released in the steam-air mixture. However, in the latter tests, steam was consumed; hence the produced hydrogen must be absorbed by the metal. It is well known that zirconium can dissolve large amounts of hydrogen especially in the temperature range investigated [21] [22]. The solubility of hydrogen in the oxide is by orders of magnitude lower compared to the metal. That's why the absorbed hydrogen should be released during progressing oxidation. Of course, it cannot be excluded that hydrogen was also released during oxidation in the steam-air atmosphere, but then it must have directly recombined with oxygen and produced water.

The strong hydrogen production in steam-nitrogen atmosphere seems to have an effect on the oxidation mechanism. It reduces the oxygen partial pressure over a larger region in the porous ZrO_2/ZrN mixture compared to air and hence stabilises zirconium nitride. This may enhance the degrading effect of nitrogen and with it the oxidation kinetics, and it corresponds with the findings from the mass gain results. Furthermore, hydrogen may be responsible for the dark colour of the oxide formed in steam-nitrogen atmosphere by supporting the formation of more sub-stoichiometric oxide.

The special advantage of the experiments presented here is that per test condition a number of samples were available for post-test examinations and not only one sample at the end of the longest oxidation time as usually obtained for thermogravimetric tests. Hence, the development of the oxidation and especially of the nitrogen-affected zones could be made visible. For all nitrogen-containing atmospheres the nitrogen attack started locally after approx. 60, 20, and 5 min for temperatures of 900, 1000, and 1100°C, respectively. The increasing affected area of porous, non-protecting oxide resulted in not only linear global kinetics after transition but even increasing ones as could be clearly seen e.g. from the development of the hydrogen release rate in Figure 2e. Such kind of kinetics with nucleation and growth of porous oxide regions was already described and modelled by Lasserre for experiments with Zircaloy-4 in air at 850°C [12] [18].

The metallographic analysis of the samples showed, most pronounced for the tests at 1100°C, quite different oxidation behaviour of the inner and outer sample surfaces. Most probably this was caused by different gas flow conditions inside and outside the tube segments. It is known that the oxidation of zirconium alloys in nitrogen-containing atmospheres strongly depends on the experimental conditions (flow rates, partial pressures, availability of inert gas, etc.) influencing the local oxygen/steam availability at the surface and/or metal-oxide interface and hence the conditions for the formation of zirconium nitride [16]. Even the samples were positioned parallel to the gas flow in the furnace tube, the gas flow inside, i.e. in the gap between sample holder stick and sample, is expected to be reduced compared to outside of the tube segment.

5. Summary

124 oxidation experiments with Zircaloy-4 cladding tube segments at 900, 1000, and 1100°C have been conducted in four different atmospheres including steam, oxygen and nitrogen. The oxidation kinetics in the nitrogen-containing gas mixtures were significantly higher compared to the kinetics in steam as reference. As known already before, the formation and re-oxidation of zirconium nitride causing extremely porous and non-protective oxide scales, is the main reason for the enhanced reaction rates in nitrogen-containing atmospheres. The study demonstrated the initially local attack of nitrogen, progressively spreading on the whole surface of the sample. Gas analyses gave additional insight into the reaction mechanisms. No hydrogen release was detected in steam-air, but steam consumption indicated hydrogen absorption by the metal phase.
The extensive set of samples is available for more sophisticated post-test examinations.

Acknowledgement

The authors are grateful for technical support given by Ulrike Stegmaier and Petra Severloh (KIT) during test conduct and metallographic post-test analyses.

References

[1] G. Schanz, B. Adroguer, and A. Volchek, "Advanced treatment of zircaloy cladding high-temperature oxidation in severe accident code calculations Part I. Experimental database and basic modeling," *Nuclear Engineering and Design*, vol. 232, pp. 75-84, 2004.

[2] D.A. Powers, L.N. Kmetyk, and R.C. Schmidt, "A review of technical issues of air ingression during severe reactor accidents," 1994.

[3] J. Fleurot et al., "Synthesis of spent fuel pool accident assessments using severe accident codes," *Annals of Nuclear Energy*, vol. 74, pp. 58-71, 2014.

[4] V. Riikonena, V. Kouhiaa, O.-P. Kauppinena, H. Sjövallb, and J. Hyvärinena, "Experimental observation of adverse and beneficial effects of nitrogen on reactor core cooling," *Nuclear Engineering and Design*, vol. 332, pp. 111–118, 2018.

[5] E.B. Evans, N. Tsangarakis, H.B. Probst, and N.J. Garibotti, "Critical role of nitrogen during high temperature scaling of zirconium," in *Proceedings of the Metallurgical Society of AIME Symposium on High Temperature Gas–Metal Reactions in Mixed Environments, 9–10 May 1972*, Boston, 1972, pp. 248-281.

[6] C.J. Rosa and W.W. Smeltzer, "The oxidation of zirconium on oxygen-nitrogen atmospheres," *Zeitschrift für Metallkunde*, vol. 71, pp. 470-475, 1980.

[7] M. Steinbrück et al., "Experiments on air ingress during severe accidents in LWRs," *Nuclear Engineering and Design*, vol. 236, pp. 1709-1719, 2006.

[8] C. Duriez et al., "Separate-effect tests on zirconium cladding degradation in air ingress situations," *Nuclear Engineering and Design*, vol. 239, pp. 244-253, 2009.

[9] M. Steinbrück, "Prototypical experiments relating to air oxidation of Zircaloy-4 at high temperatures," *Journal of Nuclear Materials*, vol. 392, pp. 531-544, 2009.

[10] M. Steinbrück and M. Böttcher, "Air oxidation of Zircaloy-4, M5® and ZIRLO™ cladding alloys at high temperatures," *Journal of Nuclear Materials*, vol. 414, pp. 276-285, 2011.

[11] C. Duriez, D. Drouan, and G. Pouzadoux, "Reaction in air and in nitrogen of pre-oxidised Zircaloy-4 and M5™ claddings," *Journal of Nuclear Materials*, vol. 441, pp. 84-95, 2013.

[12] M. Lasserre et al., "Qualitative analysis of zircaloy-4 cladding air degradation in O 2-N2 mixtures at high temperature," *Materials and Corrosion*, vol. 65, pp. 250-259, 2014.

[13] M. Steinbrück and M. Grosse, "Deviations from parabolic kinetics during oxidation of zirconium alloys," *ASTM Special Technical Publication*, vol. STP 1543, pp. 979-1001, 2015.

[14] M. Steinbrück and S. Schaffer, "High-Temperature Oxidation of Zircaloy-4 in Oxygen–Nitrogen Mixtures," *Oxidation of Metals*, vol. 85, pp. 245-262, 2015.

[15] M. Steinbrück, F.O. da Silva, and M. Grosse, "Oxidation of Zircaloy-4 in steam-nitrogen mixtures at 600–1200 °C," *Journal of Nuclear Materials*, vol. 490, pp. 226-237, 2017.

[16] M. Grosse, M. Steinbrueck, Y. Maeng, and J. Sung, "Influence of the steam and oxygen flow rate on the reaction of zirconium in steam/nitrogen and oxygen/nitrogen atmospheres," in *International Congress on Advances in Nuclear Power Plants, ICAPP*, San Francisco, 2016, pp. 2103-2111.

[17] M. Steinbrück, "High-temperature reaction of oxygen-stabilized α-Zr(O) with nitrogen," *Journal of Nuclear Materials*, vol. 447, pp. 46-55, 2014.

[18] M. Lasserre et al., "Modelling of Zircaloy-4 accelerated degradation kinetics in nitrogen-oxygen mixtures at 850 °C," *Journal of Nuclear Materials*, vol. 462, pp. 221-229, 2015.

[19] J.H. Baek and Y.H. Jeong, "Breakaway phenomenon of Zr-based alloys during a high-temperature oxidation," *Journal of Nuclear Materials*, vol. 372, pp. 152–159, 2008.

[20] R.E. Pawel, J.V. Cathcart, and R.A. McKee, "The Kinetics of Oxidation of Zircaloy-4 in Steam at High Temperatures," *Journal of the Electrochemical Society*, vol. 126, pp. 1105-1111, 1979.

[21] M. Steinbrück, "Hydrogen absorption by zirconium alloys at high temperatures," *Journal of Nuclear Materials*, vol. 334, pp. 58-64, 2004.

[22] M. Große, E. Lehmann, M. Steinbrück, G. Kühne, and J. Stuckert, "Influence of oxide layer morphology on hydrogen concentration in tin and niobium containing zirconium alloys after high temperature steam oxidation," *Journal of Nuclear Materials*, vol. 385, pp. 339-345, 2009.